

A two-fold interpenetrated flexible bi-pillared-layer framework of Fe(II) with interesting solvent adsorption property

RITESH HALDAR^a and TAPAS KUMAR MAJI^{a,b,*}

Molecular Materials Laboratory, ^aNew Chemistry Unit and ^bChemistry and Physics of Materials Unit, Jawaharlal Nehru Centre for Advanced Scientific Research, Jakkur, Bangalore 560064, India
e-mail: tmaji@jncasr.ac.in

Abstract. A two-fold interpenetrated microporous bi-pillared-layer framework of Fe(II), {[Fe(2,6-napdc)(4,4'-bipy)](EtOH)(H₂O)}_n (**1**) (2,6-napdc = 2,6-naphthalenedicarboxylate; 4,4'-bipy = 4,4'-bipyridine) composed of mixed ligand system has been synthesized and structurally characterized. The 2,6-napdc linkers form a 2D corrugated sheet of {Fe(2,6-napdc)}_n by linking the secondary building unit of Fe₂(CO₂)₂ in the *ac* plane, which are further connected by double 4,4'-bipy pillars resulting in a bi-pillared-layer type 3D framework. The 3D framework is two-fold interpenetrated and exhibits a 3D channel structure (4.0 × 3.5, 1.5 × 0.5 and 2.2 × 2.1 Å²) occupied by the guest water and ethanol molecules. Framework **1** shows high thermal stability, and the desolvated framework (**1'**) renders permanent porosity realized by N₂ adsorption profile at 77 K (BET surface area of ~52 m² g⁻¹). Moreover, the framework **1'** also uptakes different solvent vapours (water, methanol and ethanol) and their type-I profile suggest strong interaction with pore surfaces and overall hydrophilic nature of the framework. Temperature dependent magnetic measurements suggest overall antiferromagnetic behaviour in compound **1**.

Keywords. Fe(II)-MOF; bi-pillared-layer structure; interpenetration; porous framework; vapour adsorption.

1. Introduction

During the last couple of decades a new class of materials, namely metal-organic frameworks (MOFs) or porous coordination polymers (PCPs) has been one of the most highlighted materials due to the versatile functionalities.^{1–6} MOFs have been found more superior over other porous materials like zeolites, activated carbons^{7–10} in terms of their tunable porosity, structural versatility and flexible properties. Excluding gas storage and separation in MOFs,^{11–17} several other interesting properties and applications have been unveiled which include catalysis,^{18–20} ion exchange,^{21,22} magnetism,^{23–27} optical^{28–30} and even drug delivery.³¹ Because of the enormous possibilities of combining different metals and various organic linkers, it is feasible to design wide range of MOFs structure which is found in the current literature. The geometry of the metal ions and the binding mode and polarity of the linkers play significant roles on the overall topology and functionalities in MOFs. However, the rational synthesis of such framework is often baffled by interpenetration and architectural frailness; arise

from the presence of long organic struts which extend into the distances between the metal centres. Therefore, control over interpenetration, which is impediments to porous properties, is an important challenge in the field of crystal engineering. To some extent, by judicious choice of linkers and by large template molecules the framework interpenetration would be nullified.^{32–35} However, there are several recent reports on interpenetrated frameworks exhibit interesting porous properties, especially guest-induced dynamic behaviour based on sliding between the interpenetrated nets.^{5,11,36} In general, interpenetration decreases the channel size significantly which renders effective space for small molecule like hydrogen by increasing strength of interaction in an entrapment mechanism.⁵ Lately, we have demonstrated a three-fold interpenetrated Cu(II) frameworks with good amount of hydrogen uptake where the density of adsorbed hydrogen is comparable to the liquid hydrogen density.⁴ In this context, to our surprise metal-organic framework based on Fe(II) is relatively less explored, probably due to instability of Fe(II) in aerobic condition.^{36–39} Although Fe(II) exhibits versatile geometry, it may show interesting guest-induced magnetic and redox properties.³⁶

In this paper, we report synthesis, structural characterization, and adsorption properties of a 3D porous

*For correspondence

framework $\{[\text{Fe}(2,6\text{-napdc})(4,4'\text{-bipy})](\text{EtOH})(\text{H}_2\text{O})\}_n$ (**1**) [2,6-napdc = 2,6-naphthalenedicarboxylate, 4,4'-bipy = 4,4'-bipyridine] built by mixed ligand system. Upon two-fold interpenetration framework provides a 3D channel structure occupied by the guest water and ethanol molecules. The dehydrated framework shows structural transformation suggesting flexibility in the framework and also realized by the different solvent (water, methanol and ethanol) adsorption studies. The dehydrated framework possesses a BET surface area of $\sim 52 \text{ m}^2 \text{ g}^{-1}$. The temperature dependent magnetic measurements suggest overall antiferromagnetic behaviour in compound **1**.

2. Experimental

2.1 Materials

All the reagents employed were commercially available and used as provided without further purification. All the metal salts were obtained from Spectrochem, 2,6-naphthalenedicarboxylate and 4,4'-bipyridine were obtained from Sigma Aldrich chemicals.

2.2 Synthesis of $\{[\text{Fe}(2,6\text{-napdc})(4,4'\text{-bipy})](\text{EtOH})(\text{H}_2\text{O})\}_n$ (**1**)

An aqueous solution (50 mL) of Na_2 -2,6-napdc (1 mmol, 0.260 g) was mixed with ethanolic solution (50 mL) of bipy (1 mmol, 0.156 g) and the resulting solution was stirred for 30 min to mix well. $\text{FeCl}_2 \cdot 4\text{H}_2\text{O}$ (1 mmol, 0.111 g) was dissolved in 100 mL water and 2 mL of this Fe(II) solution was slowly and carefully layered with the above mixed ligand solution using 1 mL buffer (1:2 of water and EtOH) solution. Deep brown square block shaped crystals were obtained after one month. Crystals were separated and washed with EtOH/water (1:1) mixture and air dried. Bulk powder sample was prepared by the direct mixing of the respective reagent in $\text{H}_2\text{O}/\text{EtOH}$ medium under continuous flow of N_2 gas and phase purity was confirmed by the elemental analysis and PXRD patterns. Yield: 69%, Anal. Calcd. for $\text{C}_{24}\text{H}_{21}\text{FeN}_2\text{O}_6$: C, 58.89; H, 4.29; N, 5.73. Found: C, 58.13; H, 4.17; N, 5.01. FT-IR (KBr pellet, 4000–400 cm^{-1}): 3560 (s), 2954 (m) 1614(S), 1433(S), 1346(m), 1321(m), 840(m).

2.3 Physical measurements

The elemental analysis was carried out using a Thermo Fischer Flash 2000 Elemental Analyzer. IR spectrum

was recorded on a Bruker IFS 66v/S spectrophotometer with samples prepared in KBr pellets in the region 4000–400 cm^{-1} . Thermogravimetric analysis (TGA) was carried out (Metler Toledo) in nitrogen atmosphere (flow rate = 50 ml min^{-1}) in the temperature range 30–500°C (heating rate = 3°C min^{-1}). Powder XRD pattern of the products were recorded by using Mo-K_α radiation (Bruker D8 Discover; 40 kV, 30 Ma). The pattern agreed with those calculated from single crystal structure determination. Magnetic property of the sample was measured using a vibrating sample magnetometer in SQUID, the Magnetic Property Measurement System (MPMS) under zero-field-cooled (ZFC) condition in the temperature range of 300–2 K under a magnetic field of 500 Oe.

2.4 X-ray crystallography

A suitable single crystal of **1** was mounted on a glass fibre and coated with epoxy resin and X-ray data was collected on a Rigaku Mercury Diffractometer with graphite monochromated Mo-K_α radiation ($\lambda = 0.71069 \text{ \AA}$) equipped with a CCD 2D detector. The size of the unit cell was calculated from the reflections collected on the setting angles of seven frames by changing of 0.5° for each frame. Three different settings were used and were changed by 0.5° per frame and intensity data were collected with a scan width of 0.5°. Empirical absorption correction by using REQABA was performed.⁴⁰ Structure of **1** was solved by direct methods using SIR-92 program⁴¹ and expanded by using Fourier techniques.⁴² The non-hydrogen atoms were refined anisotropically and all hydrogen atoms placed in the ideal positions. All calculations were carried out using SHELXS 97,⁴³ PLATON 99,⁴⁴ and WinGX system, Ver 1.70.01.⁴⁵ Potential solvent accessible area or void space was calculated using the PLATON⁴⁴ multi-purpose crystallographic software. All crystallographic and structure refinement parameters are summarized in table 1. Selected bond lengths and angles are displayed in table 2.

2.5 Adsorption study

The adsorption isotherm of N_2 (77 K) using the dehydrated sample of **1** was measured by using QUANTACHROME QUADRASORB-SI analyzer. In the sample tube the adsorbent sample **1** (~ 100 – 150 mg) was placed which had been prepared at 393 K under a $1 \times 10^{-1} \text{ Pa}$ vacuum for about 10 h prior to measurement of the isotherms. Helium gas (99.999% purity) at a

Table 1. Crystal data and structure refinement parameters of compound **1**.

| Parameters | 1 |
|--|---|
| Empirical formula | C ₂₄ H ₂₁ N ₂ FeO ₆ |
| <i>M</i> | 489.26 |
| Cryst. system | Orthorhombic |
| Space group | <i>Pcca</i> (No. 54) |
| <i>a</i> (Å) | 24.451(7) |
| <i>b</i> (Å) | 11.479(3) |
| <i>c</i> (Å) | 16.299(4) |
| <i>V</i> (Å ³) | 4575(2) |
| <i>Z</i> | 8 |
| <i>T</i> (K) | 293 |
| λ (Mo K _α) | 0.71073 |
| <i>D_c</i> (g cm ⁻³) | 1.415 |
| μ (mm ⁻¹) | 0.702 |
| θ _{max} (deg) | 27.5 |
| Total data | 5203 |
| Unique reflection | 2576 |
| <i>R</i> _{int} | 0.076 |
| Data [<i>I</i> > 2σ(<i>I</i>)] | 2577 |
| <i>R</i> ^{<i>a</i>} | 0.0654 |
| <i>R</i> _w ^{<i>b</i>} | 0.1499 |
| GOF | 0.96 |

certain pressure was introduced in the gas chamber and allowed to diffuse into the sample chamber by opening the valve. The amount of gas adsorbed was calculated readily from pressure difference ($P_{cal} - P_e$), where P_{cal} is the calculated pressure with no gas adsorption and P_e is the observed equilibrium pressure. All operations were computer-controlled and automatic.

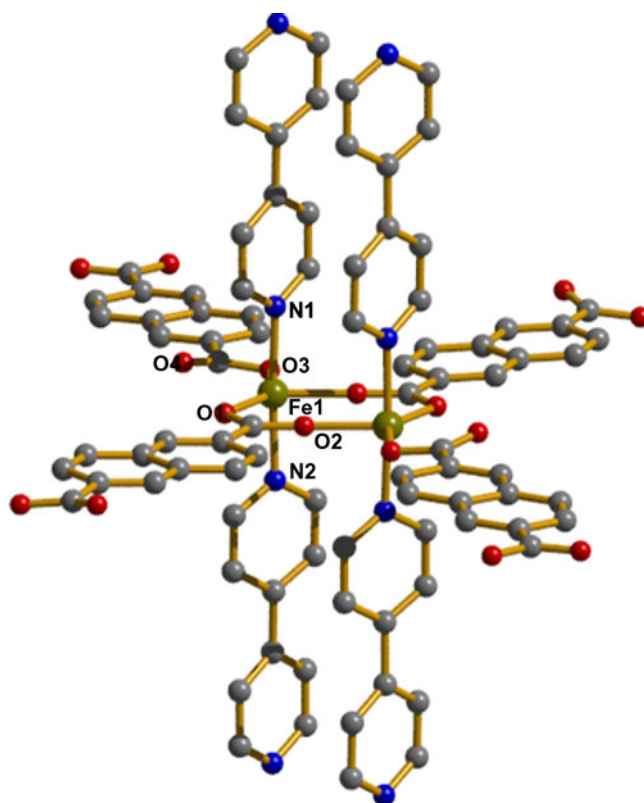
The adsorption of different solvents like methanol (MeOH) at 293 K and water (H₂O), ethanol (EtOH) at 298 K were measured in the vapor state by using BELSORP-aqua-3 analyzer. In all the measurements, in the sample tube adsorbent compound **1** (~100–150 mg) was placed which was prepared by heating **1** at 393 K for about 10 hours under vacuum prior to measurement of the isotherms. The different solvent molecules used to generate the vapour were degassed fully by repeated evacuation. Dead volume was measured with helium gas. The adsorbate was placed into the sample tube,

then the change of the pressure was monitored and the degree of adsorption was determined by the decrease in pressure at the equilibrium state. All operations were computer-controlled and automatic.

3. Results and discussion

3.1 Structural description of {[Fe(2,6-napdc)(4,4'-bipy)](EtOH)(H₂O)}_n (**1**)

Compound **1** crystallizes in orthorhombic *Pcca* space group and X-ray single crystal structure determination shows a 3D coordination framework of Fe(II) bridged by the 2,6-napdc and 4,4'-bipy linkers. In **1** each Fe(II) connected to the three different oxygen atoms (O1, O2_b and O4_d; $b = 1 - x, y, 3/2 - z$; $d = 1/2 + x, y, 1 - z$) from the three different 2,6-napdc linkers in the equatorial positions and the axial positions are occupied by the two nitrogen atoms (N1, N2) from two different 4,4'-bipy pillars (figure 1). Therefore, each Fe(II) is in a trigonal bipyramidal geometry with FeO₃N₂ chromosphere. Fe1–O and Fe1–N bond distances are in the range of 2.026(3)–2.048(3) Å and 2.165(4)–2.189(4) Å, respectively. The distortion from the perfect

**Figure 1.** View of the coordination environment around Fe(II) and the building unit in framework **1**.**Table 2.** Selected bond lengths (Å) and angles (°) for **1**.

| | | | |
|-------------|------------|---------------|------------|
| Fe1–O1 | 2.048(3) | Fe1–N1 | 2.165(4) |
| Fe1–O2_b | 2.026(3) | Fe1–O4_d | 2.068(3) |
| O1–Fe1–N1 | 89.35(13) | O1–Fe1–O2_b | 126.00(14) |
| O1–Fe1–O4_d | 143.20(13) | O2_b–Fe1–N1 | 88.29(16) |
| O4_d–Fe1–N1 | 90.98(15) | O2_b–Fe1–O4_d | 90.79(14) |

Symmetry code: $b = 1 - x, y, 3/2 - z$; $d = 1/2 + x, y, 1 - z$

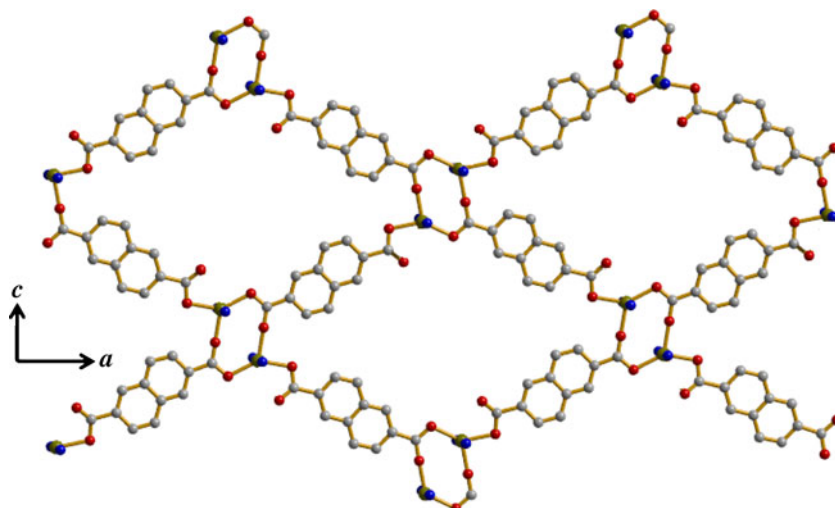


Figure 2. 2D sheet of $\{\text{Fe}_2(2,6\text{-napdc})_2\}_n$ along crystallographic ac plane.

TBP geometry around each Fe(II) is reflected in the *cisoid* angles ($88.29(16)$ – $90.98(15)^\circ$). Two 2,6-napdc connect two Fe(II) atoms in a *syn-syn* fashion forming $\text{Fe}_2(\text{CO}_2)_2$ secondary building unit (SBU) and each binuclear core connected by another two 2,6-napdc by the monodentate carboxylate oxygen (O4) atom forming a perfectly 2D planar $[\text{Fe}_2(2,6\text{-napdc})_2]_n$ sheet lying in the crystallographic ac plane (figure 2). Each 2D sheet further pillared by the 4,4'-bipy resulting a 3D pillared layer network. It is worth to mention that the two Fe(II) centers of the binuclear $\text{Fe}(\text{CO}_2)_2$ core in the 2D sheet are pillared by the double column of 4,4'-bipy forming a bi-pillared-layer framework (figure 3). Two 3D frameworks are mutually two-fold interpenetrated resulting in a two-fold interpenetrated 3D framework with three-dimensional channels occupied by the guest molecules (figure 4). Along the a , b and c -axis (figure 4) the dimension of the channels are 2.0×0.5 , 1.5×0.5 and $4.0 \times 3.5 \text{ \AA}^2$,⁴⁶ all provide 25.9% void space to the total crystal volume (figure 5). Along the c axis rectangular shaped channels are occupied by the H_2O and EtOH molecules; however, along the b axis small banana-shaped channels are occupied by the H_2O molecules (figure 4). In the dinuclear core the Fe...Fe separation is 3.858 \AA and along the 2,6-napdc and 4,4'-bipy Fe...Fe separation are 12.892 and 11.479 \AA , respectively.

3.2 TG analysis and PXRD

To examine the thermal stability of the framework thermal gravimetric (TG) analysis and powder X-ray diffraction (PXRD) measurements were carried out.

TGA curve (figure S1) shows the release of the guest H_2O and EtOH molecules up to 120°C to give the desolvated form $\{[\text{Fe}(2,6\text{-napdc})(4,4'\text{-bipy})]\}_n$ (**1'**) which is stable up to 220°C without further weight loss. On further heating, the compound decomposes to unidentified product. PXRD pattern of the desolvated state shows some changes in Bragg intensity and peak positions compared to the as-synthesized framework suggesting structural changes after removal of the guest molecules (figure S2).

3.3 Adsorption study

The three-dimensional compound **1** has been subjected to study the porous properties after activating at

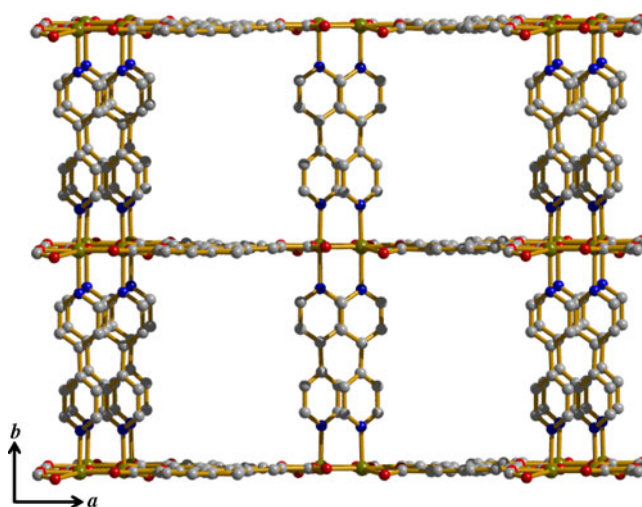


Figure 3. View of the 3D bi-pillared-layer framework of **1**.

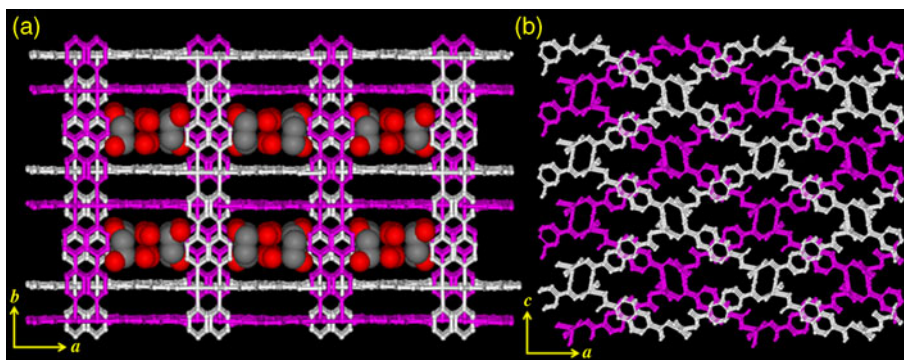


Figure 4. (a) View of the two-fold interpenetrated framework along the crystallographic *c*-axis with rectangular channels occupied by the guest water and ethanol molecules; (b) view of the interpenetrated framework along the crystallographic *b*-axis.

120°C for 10 h under vacuum. A N₂ (kinetic diameter; 3.64 Å)⁴⁷ adsorption was carried out at 77 K as shown in figure 6. The adsorption isotherm displays a rapid rise at low relative pressure followed by a monotonically increasing profile with the increasing of pressure and ended with the adsorption amount of 73 mL g⁻¹. The corresponding Brunauer–Emmet–Teller (BET) surface area is about 52 m² g⁻¹. The surface area is smaller than expected on the basis of the crystal structure, a fact that is attributed to the small amount of adsorption at low relative pressure. Regardless of the stable framework and larger pore diameter, the effective N₂ diffusion into the micropore was not observed. This is probably due

to the pore blocking at low temperature or dynamic movement of the interpenetrated net which hindered N₂ molecules passing into the pore efficaciously as observed in other porous coordination framework.¹¹ Figure 7 shows H₂O (2.65 Å), MeOH (3.8 Å) and EtOH (4.3 Å) adsorption isotherms at 298 K. In spite of the difference in saturation amounts among the solvent uptake, all the isotherms exhibit type-I curves which are indicative of typical micropores. H₂O adsorption profile shows a steep uptake at low pressure and then saturates with an uptake amount of ~57 mL g⁻¹ (1.2 molecules per formula). Though MeOH molecule has comparatively larger, the kinetic diameter uptake amount is

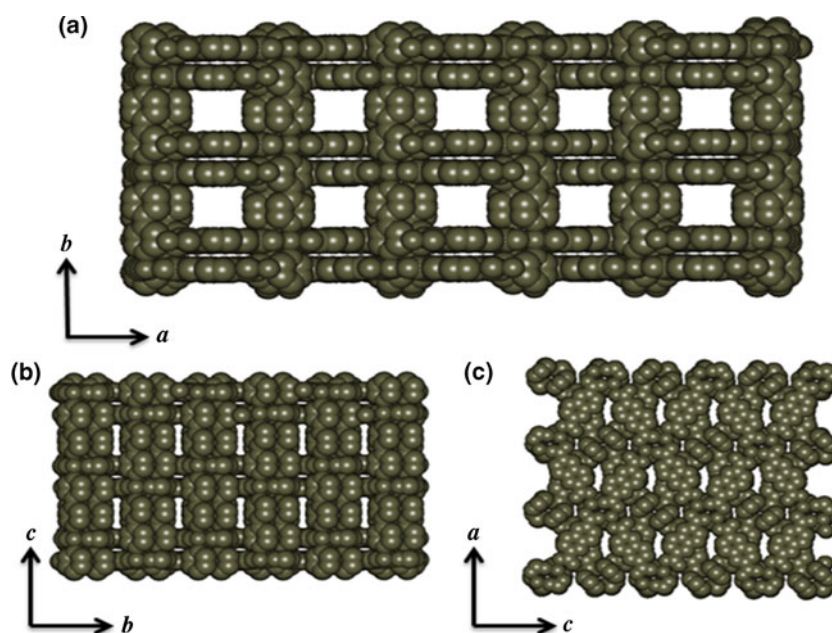


Figure 5. CPK diagram of **1** showing the channels (a) along *c* axis, (b) along *a* axis, (c) along *b* axis.

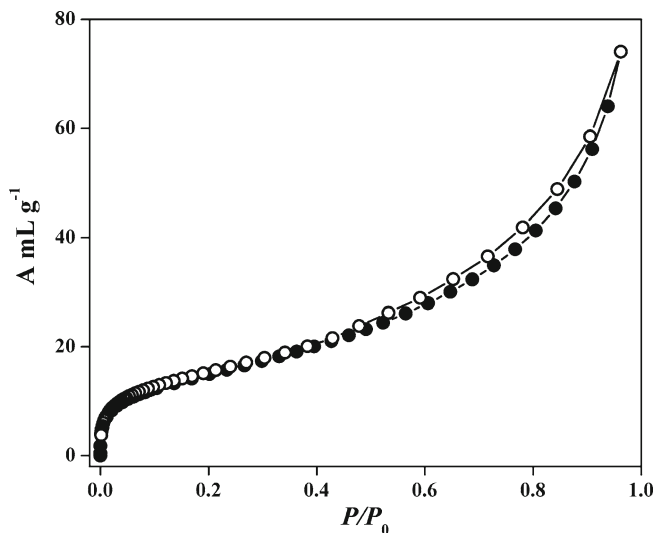


Figure 6. N_2 adsorption isotherm at 77 K for the desolvated compound of **1**.

close to that of H_2O and per formula unit about one MeOH molecule occluded. Final uptake volume of EtOH indicates about ~ 0.7 molecule has been adsorbed by the framework. The overall adsorption behaviour indicates that the pore surfaces are rather hydrophilic in nature realized by the βE_o values (4.5 kJ/mol for H_2O ; 3.9 kJ/mol for MeOH and 3.6 kJ/mol for EtOH) and strong interaction with the pore surfaces evoked by the hysteretic sorption profile.

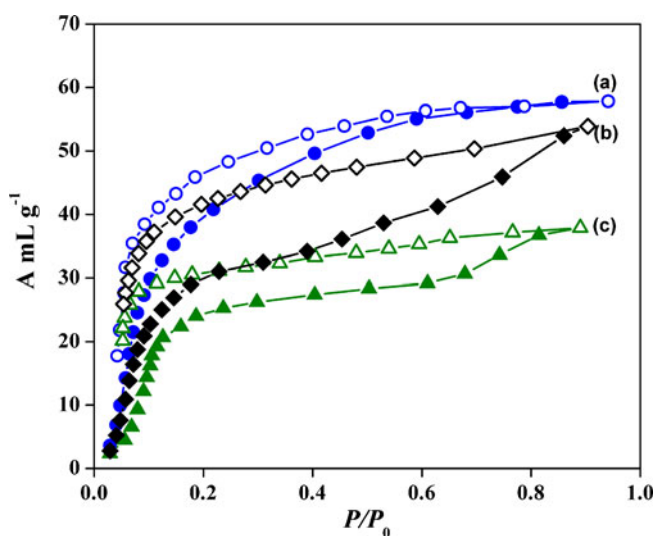


Figure 7. Vapour adsorption-desorption isotherm for desolvated compound of **1**; (a) Water at 298 K, (b) MeOH at 293 K and (c) EtOH at 298 K; P_0 is the saturated vapour pressure; 3.17 kPa (H_2O), 16.94 kPa (MeOH), 7.87 kPa (EtOH); (filled circle: adsorption, open circle: desorption).

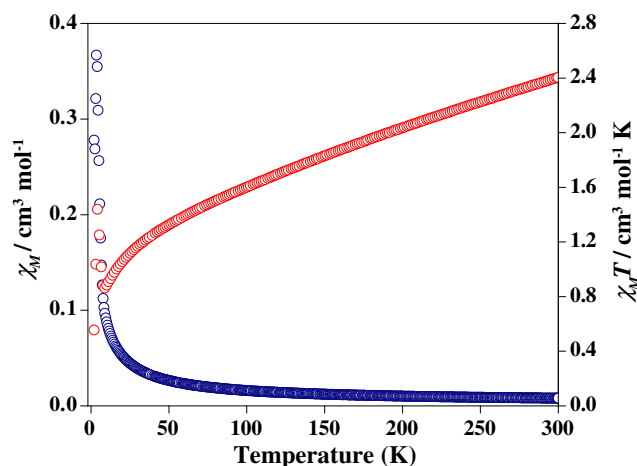


Figure 8. Temperature dependence χ_M (blue) and $\chi_M T$ (red) plots for compound **1**.

3.4 Magnetic property of $\{[Fe(2,6\text{-napdc})(4,4'\text{-bipy})](EtOH)(H_2O)]_n\}$ (**1**)

Magnetic measurement was carried out on a crystalline powder sample of compound **1**. The magnetic susceptibility data collected in the temperature range of 300–2 K under an applied field of 500 Oe and the plots of χ_M vs T and $\chi_M T$ vs T are shown in figure 8. The χ_M value at 300 K is $0.00828 \text{ cm}^3 \text{ mol}^{-1}$ ($\chi_M T = 2.484 \text{ cm}^3 \text{ mol}^{-1} \text{ K}$) which agrees well with the expected spin only value of Fe(II).^{48,49} The $\chi_M T$ value continuously decreases from $2.484 \text{ cm}^3 \text{ mol}^{-1} \text{ K}$ at 300 K to $0.861 \text{ cm}^3 \text{ mol}^{-1} \text{ K}$ at 8 K suggesting an overall antiferromagnetic behaviour. Below this temperature there is a sharp enhancement and $\chi_M T$ value reaches a maximum value of $1.439 \text{ cm}^3 \text{ mol}^{-1} \text{ K}$, and further it drops down to $0.555 \text{ cm}^3 \text{ mol}^{-1} \text{ K}$, suggesting weak ferromagnetic interaction at low temperature in compound **1**. A plot of $1/\chi_M$ vs T in the temperature range 300–130 K obeys Curie-Weiss law with a Weiss constant $\theta = -141.99 \text{ K}$ (figure S3), suggesting antiferromagnetic interaction operating between the Fe(II) centers.

4. Conclusion

In conclusion, we have successfully synthesized and characterized a 3D bipillered-layer porous two-fold interpenetrated Fe(II) framework with mixed ligand system. It represents a unique MOF based on +2 oxidation state of iron with high thermal stability, structural flexibility and interesting solvent adsorption properties. This work unveiled that the large template molecule like ethanol decreases the number of interpenetrating net as

with same set of linkers without template molecules display three-fold interpenetration in Cu(II) system.⁴ Therefore, the judicious choice of linkers, metal ions and template molecules is of significance for fabricating the desired framework structure.

Supplementary data

Tables of X-ray crystallographic data in CIF format for the structures reported in this paper have been deposited to the Cambridge Crystallographic Data Center, CCDC number is 834911. Copies of this information may be obtained free of charge from the Director, CCDC, 12 Union Road, Cambridge CB2 1EZ, UK [fax: C44 1223 336033; e-mail: deposit@ccdc.cam.ac.uk Web: <http://www.ccdc.cam.ac.uk/deposit>]. Supplementary figures S1–S3 can be found in the Journal of Chemical Sciences Website (www.ias.ernet.in/chemsci).

Acknowledgements

TKM gratefully acknowledges the financial support from the Department of Science and Technology (DST), Govt. of India (Fast Track Proposal). RH acknowledges DST and Jawaharlal Nehru Centre for Advanced Scientific Research (JNCASR), Bangalore, India.

References

- Kitagawa S, Kitaura R and Noro S-I 2004 *Angew. Chem. Int. Ed.* **43** 2334
- Férey G 2008 *Chem. Soc. Rev.* **37** 191
- Eddaoudi M, Moler D B, Li H L, Chen B L, Reineke T M, O'Keeffe M and Yaghi O M 2001 *Acc. Chem. Res.* **34** 319
- Kanoo P, Matsuda R, Higuchi M, Kitagawa S and Maji T K 2009 *Chem. Mater.* **21** 5861
- Ma S, Sun D, Ambrogio M, Fillinger J A, Parkin S and Zhou H-C 2007 *J. Am. Chem. Soc.* **129** 1858
- Hazra A, Kanoo P and Maji T K 2011 *Chem. Commun.* **47** 538
- Belmabkhout Y and Sayari A 2009 *Adsorption* **15** 318
- Kim B J, Cho K S and Park S J 2010 *J. Colloid Interface Sci.* **342** 575
- Zukal A, Dominguez I, Mayerová J and Cezka J 2009 *Langmuir* **25** 10314
- Kim S N, Son W J, Choi J S and Ahn W S 2008 *Microporous Mesoporous Mater.* **116** 394
- Maji T K, Matsuda R and Kitagawa S 2007 *Nat. Mater.* **6** 142
- Wang Z Q and Cohen S M 2009 *J. Am. Chem. Soc.* **131** 16675
- Mohapatra S, Hembram K P S S, Waghmore U and Maji T K 2009 *Chem. Mater.* **21** 5406
- Matsuda R, Kitaura R, Kitagawa S, Kubota Y, Belosludov R V, Kobayashi T C, Sakamoto H, Chiba T, Takata M, Kawazoe Y and Mita Y 2005 *Nature* **436** 238
- Choi H J, Dincá M and Long J R 2008 *J. Am. Chem. Soc.* **130** 7848
- Kanoo P, Haldar R, Cyriac S T and Maji T K 2011 *Chem. Commun.* **47** 11038
- Dey R, Haldar R, Maji T K and Ghoshal D 2011 *Cryst. Growth Des.* **11** 3905
- Venna S R and Carreon M A 2010 *J. Am. Chem. Soc.* **132** 76
- Xia M H, Yang X L, Zou C and Wu C D 2011 *Inorg. Chem.* **50** 5318
- Colombo V, Galli S, Choi H J, Han G D, Maspero A, Palmisano G, Masciocchi N and Long J 2011 *Chem. Sci.* **7** 1311
- Muthu S, Yip J H K and Vittal J J 2002 *J. Chem. Soc. Dalton Trans.* **24** 4561
- Sun C Y, Liu S X, Liang D D, Shao K J, Ren Y H and Su Z M 2009 *J. Am. Chem. Soc.* **131** 1883
- Kanoo P K, Ghosh A C and Maji T K 2011 *Inorg. Chem.* **50** 400
- Centrone A, Harada T, Speakman S and Halton T A 2010 *Small* **15** 1598
- Kurmoo M 2009 *Chem. Soc. Rev.* **28** 1353
- Kanoo P K, Madhu C, Mostafa G, Maji T K, Sundaresan A, Pati S K and Rao C N R 2009 *Dalton Trans.* **38** 5062
- Lohe M R, Gedrich K, Freudenbarg T, Kockrich E, Dellmann T and Kaskel S 2011 *Chem. Commun.* **47** 3075
- Jayaramulu K, Kanoo P, George S J and Maji T K 2010 *Chem. Commun.* **46** 7906
- Cai S L, Zheng S R and Fan J 2011 *Inorg. Chem.* **6** 937
- Pramanik S, Zheng C and Zhang X 2011 *J. Am. Chem. Soc.* **133** 4153
- An J Y, Geib S J and Rosi N L 2009 *J. Am. Chem. Soc.* **131** 8376
- He H, Yuan D, Ma H, Sun D, Zhang G and Zhou H-C 2010 *Inorg. Chem.* **49** 7605
- Ma L Q and Lin W B 2008 *J. Am. Chem. Soc.* **130** 13834
- Shekhah O, Wang H, Paradinas M, Ocal C, Schupbach B, Terfort A, Zacher D, Fischer R A and Woll C 2009 *Nat. Mater.* **8** 481
- Wang Q, Zhang J Y, Zhuang C F, Tang Y and Su C Y 2009 *Inorg. Chem.* **48** 287
- Halder G J, Kepert C J, Moubaraki B, Murrey K S and Cashion J D 2002 *Science* **295** 1762
- Geisheimer A R, Huang W, Pacradouni V, Sonier J E and Leznoff D B 2011 *Dalton Trans.* **40** 7505
- Moatazedi Z, Katz M J and Leznoff D B 2010 *Dalton Trans.* **39** 9889
- Zeng M -H, Feng X -L and Chen X -M 2004 *J. Chem. Soc. Dalton Trans.* **33** 2217
- Jacobson R A, *REQABA Empirical absorption Correction Ver. 1.1-03101998*, Molecular Structure Corp., The Woodlands, TX (1996–1998)
- Altomare A, Burla M C, Camalli M, Cascarano G L, Giacovazzo C, Guagliardi A, Moltireni M G G, Polidori G and Spanga R 1999 *J. Appl. Crystallogr.* **32** 115
- Beurskens P T, Admiraal G, Beurskens G, Bosman W P, deGelder R, Israel R and Smits J M M 1994

- The DIRDIF-94 program system; technical report of the crystallography laboratory* (University Nijmegen; Nijmegen, The Netherlands)
43. Sheldrick G M SHELXL-97 1997 *Germany Program for Crystal Structure Solution and Refinement* (University of Göttingen; Göttingen)
 44. Spek A L 2003 *J. Appl. Crystallogr.* **36** 7
 45. Farrugia L J 1999 *J. Appl. Crystallogr.* **32** 83
 46. The sizes of the channels were calculated considering the van der Waals radii of the atoms
 47. Webster C E, Drago R S and Zerner M C 1998 *J. Am. Chem. Soc.* **120** 5509
 48. Li Y -W, Zhao J -P, Wang L -F and Bu X -H 2011 *Cryst. Eng. Comm.* **13** 5598
 49. Djukic B, Seda T, Gorelsky S I, Lough A J and Lemaire M T 2011 *Inorg. Chem.* **50** 7334